

3. Vincent, J. S., C. J. Steer, and I. W. Levin. 1984. Infrared spectroscopic study of the pH-dependent secondary structure of brain clathrin. *Biochemistry*. 23:625-631.
4. Huang, C. H., J. R. Lapidus, and I. W. Levin. 1982. Phase transition behavior of saturated, symmetric chain phospholipid bilayer dispersions determined by Raman spectroscopy: correlation between spectral and thermodynamical parameters. *J. Amer. Chem. Soc.* 104:5926-5930.
5. Steer, C. J., J. S. Vincent, and I. W. Levin. 1984. Membrane response to clathrin coat protein determined by infrared spectroscopy: possible involvement in coated vesicle formation. *J. Biol. Chem.* 259:8052-8055.

# NUCLEAR MAGNETIC RESONANCE, BIOCHEMICAL, AND MOLECULAR GENETIC STUDIES OF THE MEMBRANE-BOUND D-LACTATE DEHYDROGENASE OF *ESCHERICHIA COLI*

CHIEN HO, GORDON S. RULE, AND E. ANN PRATT

*Department of Biological Sciences, Carnegie-Mellon University, Pittsburgh, Pennsylvania 15213*

D-Lactate dehydrogenase (D-LDH) of *Escherichia coli* is an integral membrane protein which is activated by lipids and detergents. This flavin adenine dinucleotide (FAD)-containing enzyme catalyzes the oxidation of D-lactate in electron transfer reactions that are coupled to the active transport of various amino acids and sugars into the cell. We are carrying out a systematic investigation of D-LDH using techniques of  $^{19}\text{F}$  nuclear magnetic resonance (NMR), biochemistry, and molecular genetics. To obtain sufficient quantities of D-LDH, we have constructed a recombinant plasmid that overproduces D-LDH by 300-fold over wild-type levels. To construct mutants and to aid in the interpretation of our NMR data, we have determined the primary structure of D-LDH by nucleotide sequencing of the cloned gene (1). The protein has 571 amino acid residues and a molecular weight of 65,000.

## RESULTS AND DISCUSSION

By adding 4-, 5-, or 6-fluorotryptophan at the time of heat induction of D-LDH activity, we can incorporate high levels of these  $^{19}\text{F}$ -labeled analogs into the enzyme.  $^{19}\text{F}$  NMR spectra of these labeled proteins are shown in Fig. 1. The spectrum of 5F-Trp-labeled D-LDH shows five distinct Trp resonances, in agreement with the five Trp residues expected from the nucleotide sequence, at positions 59, 384, 407, 469, and 567. The intensities of the peaks in the spectra of 4- and 6F-Trp-labeled protein also indicate the presence of five resonances. Thus, each Trp in D-LDH must have a different environment. Also, the linewidth of each of the five resonances is different, suggesting that there are differences in the motional properties of each Trp residue.

In 100 mM lysolecithin, dipalmitoyl phosphatidylglycerol (DPPG), or dipalmitoyl phosphatidylcholine (DPPC),

the spectra of 5F-Trp-labeled D-LDH are as shown in Fig. 1. In 1% Triton X-100, we find that peak 3 shifts 0.5 ppm downfield. In 1% Triton X-100 plus 0.1% SDS, we find that peak 2 shifts 1 ppm downfield.

We have performed a number of experiments on the 5F-Trp-labeled enzyme, in the presence of lysolecithin, to determine the structural and dynamic properties of the Trp residues in D-LDH. By changing the ratios between  $\text{D}_2\text{O}$  and  $\text{H}_2\text{O}$  in the sample, we can induce a change in the  $^{19}\text{F}$  chemical shift of the fluorotryptophan. When we perform this experiment on D-LDH, we find that peaks 1, 2, and 3 show no chemical shift changes. Peaks 4 and 5 show a change in chemical shift which indicates that they are 60% (peak 4) and 100% (peak 5) exposed to the solvent. We have also observed the  $^{19}\text{F}$  resonances under conditions of broad-band proton irradiation, and we find that the five resonances are reduced in intensity by different amounts. In particular, resonances 4 and 5 show the least amount of reduction, which implies that they are the most mobile of the five Trp residues. This is consistent with the fact that resonances 4 and 5 are also exposed to the solvent.

When the substrate, D-lactate, is added to 5F-labeled enzyme, we find that peak 2 shows a large increase in linewidth and is shifted 0.5 ppm downfield. When oxalate, a competitive inhibitor, is added, there is no effect on the spectrum. This indicates that peak 2 is sensitive to reduction of the flavin but not to the binding of the substrate.

To summarize, we find that resonances 2 and 3 are sensitive to the lipid environment. Resonance 2 is also sensitive to the oxidation state of the FAD cofactor. In addition, we find that resonances 4 and 5 are on the surface of the enzyme.

The relationship between this information and an understanding of the structure and function of D-LDH is not simple. To obtain a "working model" for the structure

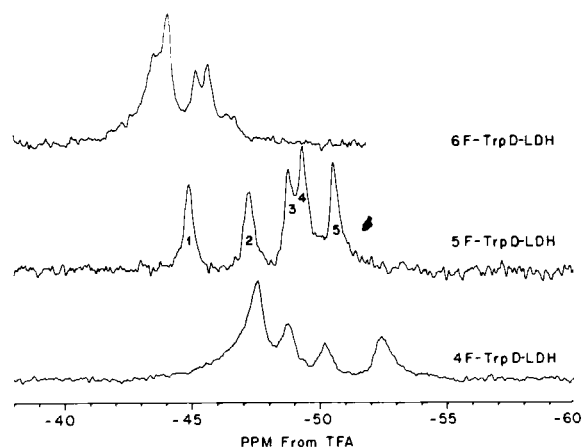
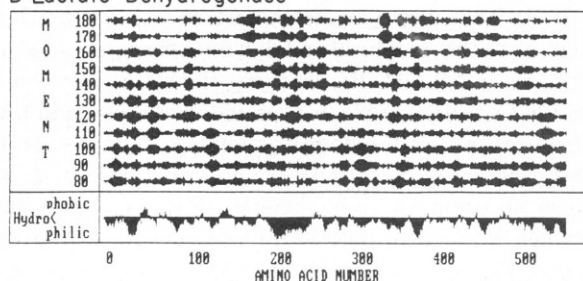


FIGURE 1  $^{19}\text{F}$  NMR spectra of 4-, 5-, and 6F-Trp-labeled D in 100 mM egg-lysolecithin, 5 mM potassium phosphate, 100  $\mu\text{M}$  EDTA at pH 7.2 and 42°C. The concentration of D-LDH was 1 mM. Spectra were obtained at 282.4 MHz on a FT NMR spectrometer. A 90° pulse of 6  $\mu\text{s}$  was used. A total of 5,000, 3,000, and 7,000 transients, respectively, were collected for the 4-, 5-, and 6F-labeled D-LDH. A line broadening of 20 Hz was applied to the free induction decay to improve the signal-to-noise ratio.

#### A. D-Lactate Dehydrogenase



#### B. Lactose Carrier Protein

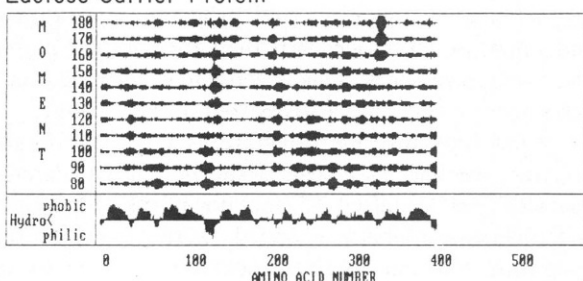


FIGURE 2 Hydrophobic moment plots are shown for D-lactate dehydrogenase (upper panel) and the lactose carrier protein (lower panel). Each panel is divided into two sections. The lower section indicates the relative hydrophobicity of the primary structure. A dark area above the midline indicates a hydrophobic region, while a dark area below the midline indicates a hydrophilic stretch of amino acids. The upper section of the panel shows the hydrophobic moment as a function of the angle (80–180°) of displacement between adjacent residues. A dark region indicates a relatively strong hydrophobic moment.

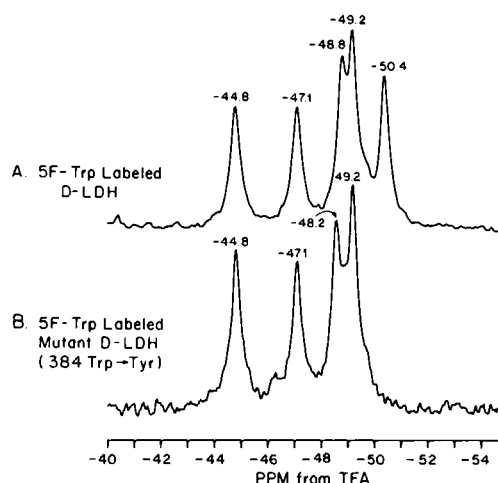


FIGURE 3  $^{19}\text{F}$  NMR spectra of wild-type and a mutant (Trp384 to Tyr) 5F-Trp-labeled D-LDH are shown. The experimental conditions are identical to those given in Fig. 1.

of D-LDH, we are using other methods of obtaining information about D-LDH. The primary sequence of the protein indicates that there are no extensive hydrophobic regions, in marked contrast to the lactose carrier protein (see Fig. 2), which contains large regions of hydrophobic amino acids. However, a hydrophobic moment analysis (2) of D-LDH (Fig. 2) indicates that there are several regions of the enzyme which could fold into amphipathic  $\alpha$  helices or  $\beta$  sheets. This implies that D-LDH is folded in such a manner that elements of secondary structure come together to form a membrane-binding domain. To support this conclusion, we have constructed a set of mutants containing small (30–60 nucleotides) in-frame deletions throughout the coding region of the D-LDH gene. We find that all of these deletions produce an inactive enzyme. This indicates that the primary sequence of D-LDH cannot be simply divided into a membrane-binding domain and a catalytic domain. We are currently extending these results by creating single nucleotide changes in the gene. This information should indicate, on a finer scale, which regions of the enzyme are important for membrane binding and catalysis.

To extend our current  $^{19}\text{F}$  NMR data, we are constructing site-specific, oligonucleotide-generated mutants. We have prepared oligomers that change each of the five Trp residues to either a Phe or a Tyr. When these synthetic oligomers are incorporated into the gene, we can prepare 5F-Trp-labeled mutant protein, and assign the  $^{19}\text{F}$  resonances to specific Trp residues in the primary sequence. Fig. 3 demonstrates that replacement of Trp384 by Tyr allows us to assign resonance 5 to Trp384.

Site-directed oligonucleotide mutagenesis is also being used to replace existing Phe or Tyr codons by Trp codons. Thus, we will be able to probe regions of D-LDH which are

not currently accessible to  $^{19}\text{F}$  NMR of F-Trp-labeled enzyme (between residues 59 and 384).

This work is supported by a research grant from the National Institutes of Health (GM-26874). G. S. Rule is supported by a training grant from the National Institutes of Health (GM-08067).

Received for publication 3 May 1985.

## REFERENCES

1. Rule, G. S., E. A. Pratt, C. C. Q. Chin, F. Wold, and C. Ho. 1985. Overproduction and nucleotide sequence of the respiratory D-lactate dehydrogenase of *Escherichia coli*. *J. Bacteriol.* 161:1059–1068.
2. Eisenberg, D., R. M. Weiss, T. C. Terwilliger, and W. Wilcox. 1982. Hydrophobic moments and protein structure. *Faraday Symp. Chem. Soc.* 17:109–120.

## PHYCOBILISOMES

### Macromolecular Structure and Energy Flow Dynamics

A. N. GLAZER\* AND J. H. CLARK†

\*Department of Microbiology and Immunology and †Laboratory of Chemical Biodynamics, Lawrence Berkeley Laboratory, and Department of Chemistry, University of California, Berkeley, California 94720

Cyanobacteria and red algae carry out efficient photosynthesis with light over the wavelength range 450 to 650 nm. The absorption of light at these wavelengths is performed by a family of intensely colored, brilliantly fluorescent chromoproteins (biliproteins). These proteins carry covalently attached open-chain tetrapyrrole (bilin) chromophores that vary in chemical structure. The chemical nature of the particular bilins attached to a given biliprotein in large measure determines its absorption spectrum. Within cyanobacterial cells and red algal chloroplasts, the biliproteins are organized into particles of intricate structure, phycobilisomes, which are attached to the outer surface of the thylakoid membrane (1).

The structure of a typical cyanobacterial phycobilisome, that of *Synechocystis* 6701, is shown in Fig. 1. The location of the various components within this structure was determined by analysis of incomplete phycobilisomes from a large number of mutants and from studies of sub-assemblies obtained by partial dissociation of phycobilisomes (1, 2). In isolated phycobilisomes, light absorbed over a wide range of wavelengths is emitted as fluorescence at ~676 nm. In intact cells, little of this emission is observed because of efficient energy-transfer from the terminal energy acceptors to two chlorophyll-*a*-containing photosystem II reaction center complexes, lying beneath the phycobilisome in the thylakoid membrane (3).

The *Synechocystis* 6701 phycobilisome is a particle of  $\sim 7.5 \times 10^6$  d that contains ~650 bilins. It is made up of two distinct kinds of substructures; rods consisting of 60 Å thick by 120 Å diameter disks of biliprotein hexamers, and a core consisting of three cylinders. The axes of the core cylinders lie at right angles to the cylindrical axes of the rods. Four rods are attached to the upper core cylinder and one rod is attached to each of the basal core cylinders. Each

of the core cylinders is made up of four 30 Å thick by 115 Å diameter "trimeric" allophycocyanin complexes. Polypeptides carrying terminal acceptor bilins,  $\alpha^{\text{APB}}$  and  $\text{L}_{\text{CM}}^{\text{99}}$  are each contained within complexes in the basal core cylinders, as illustrated in Fig. 1.

We have examined the dynamics of energy flow within complete phycobilisomes, as well as in partial structures produced by two mutants. *Synechocystis* 6701 strain CM25 produces particles lacking the two terminal phycoerythrin complexes of the rod substructures; the phycobilisome is otherwise unchanged. *Synechocystis* 6701 strain UV16 produces wild-type cores containing  $\text{L}_{\text{RC}}^{\text{27}}$  linker polypeptides, but lacking all other rod components (4). Picosecond spectroscopic studies have shown that disk-to-disk transfer (~24 ps) represents the rate-limiting step in energy flow in the rods (5). Energy transfer within the core is <11 ps.<sup>1</sup>

We have also found that within isolated biliproteins, intradisk energy transfer is very rapid, occurring in <8 ps (5). Consequently, from the standpoint of energy flow dynamics, each building block of the phycobilisome can be regarded as equivalent to a single chromophore. Because these building blocks are arranged in the order of decreasing excitation energies from the periphery of the structure to the terminal acceptors, the energy flow is highly directional towards the core. The structure of the phycobilisome also minimizes the possibilities for the random walk of excitation among like chromophores. Thus, only a small number of energy transfer steps of any significant length relative to the ~2 ns fluorescence lifetime of a biliprotein is

<sup>1</sup>Glazer, A. N., C. Chan, R. C. Williams, S. W. Yeh, and J. H. Clark. 1985. Kinetics of energy flow in the phycobilisome core. Manuscript in preparation.